Stretching Peptides

Zoë C. Adams,[‡a] Anthony P. Silvestri,[‡a] Sorina Chiorean,[a] Brian P. Balo,[a] Yifan Shi,[a] Matthew Holcomb,[b] Shawn I. Walsh,[a] Colleen A. Maillie,[b] Gregory K. Pierens,[c] Stefano Forli,[b] K. Johan Rosengren,[c] and Philip E. Dawson[a]*

[‡] Co-first author
* Corresponding author (dawson@scripps.edu)
[a] Department of Chemistry, The Scripps Research Institute, 10550 North Torrey Pines Road, La Jolla, California, USA
[b] Department of Integrated Structural and Computational Biology, The Scripps Research Institute, 10550 North Torrey Pines Road, La Jolla, California, USA
[c] Institute for Molecular Bioscience and School of Biomedical Sciences, University of Queensland, Brisbane QLD 4072, Australia

Abstract:

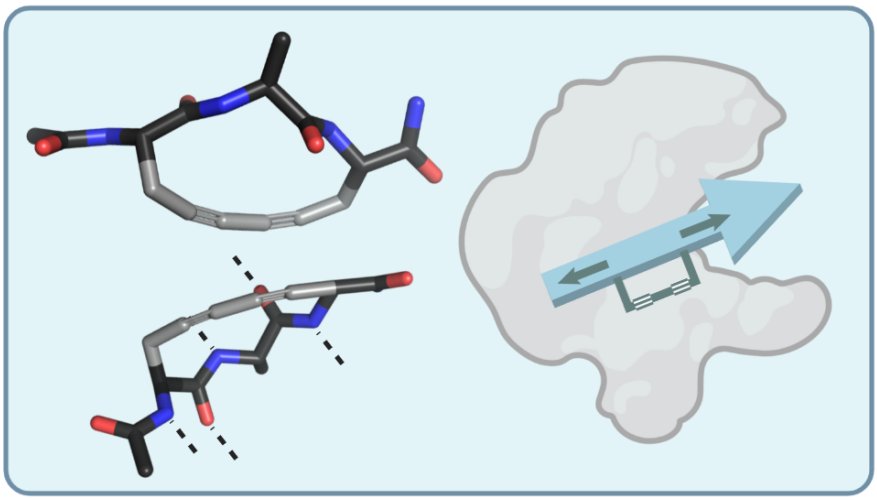

Advances in the modulation of protein-protein interactions (PPIs) enable the characterization of PPI networks that govern disease mechanisms and guide the design of novel therapeutics and probes. These PPIs are often characterized by complementary binding to shallow protein surfaces that are challenging to target using standard methods for high-affinity small molecule ligand generation. Compared to linear peptides, synthetically constrained epitopes provide an energetic advantage for binding PPI surfaces by decreasing unbound-state entropy. Such peptide stapling strategies promoting α-helix and β-hairpin structures are well developed. However, approaches for accessing common extended backbone structures are limited. Here we demonstrate the incorporation of a rigid, linear, diyne brace between side chains at the *i* to *i*+2 positions to generate a family of low molecular weight peptide macrocycles adopting extended backbones. We show by NMR and DFT studies that these 'stretched peptides' adopt rigid and stable conformations in solution which can be tuned to explore a wide range of extended peptide conformational space, including those inherent to β-strands and polyproline II (PPII) helices. The formation of the diyne brace is accomplished in excellent conversions (>95%) and is amenable to high throughput synthesis. The minimalist structure-inducing tripeptide core (< 300 Da) is amenable to further synthetic elaboration to optimize bioactivity and pharmacokinetics. We showcase the utility of diyne-braced peptides with the synthesis of macrocyclic inhibitors of bacterial signal 1 peptidase.

Introduction:

Extended amino acid backbone conformations are an abundant structural motif responsible for mediating a myriad of protein-protein interactions. Along with other secondary structures including turns and helices, extended regions present ordered backbone and side chain orientations that contribute to specific recognition of protein targets.[1-3] For example, it is estimated that over half of eukaryotic proteins contain long intrinsically disordered regions (IDRs).[4, 5] The backbone conformations of both β-strands and IDRs, which are best mimicked by type II polyproline (PPII) helices, occupy similar φ, ψ space. The development of designed peptides biased towards an extended β-strand or PPII helix conformation is relevant for solving diverse biological problems from addressing the "undruggable" population of the proteome[6-9] to modeling or disrupting peptide aggregation.[10] Chemical modification of small to medium sized synthetic peptides, including the installation of known β-turn sequences, *N*-amination of the backbone, and macrocyclization via side-chain to side-chain or side-chain to main-chain linkages,[11-18] has emerged as a powerful technique for accessing extended-backbone peptides. However, current synthetic strategies for mimicking extended structures are limited in their application since they typically require modifications that disrupt backbone hydrogen bonds defining the β-strand. Extending our studies of peptidic Glaser couplings[19] and their implementation in stapled helical peptides,[20] we investigated the incorporation of *i*, *i+2* diyne linkages into peptides as a means to construct rigid, extended-backbone peptide macrocycles. We reasoned that rather than stapling distant side chains together, stretching proximal side chains through a rigid low molecular weight linker would prevent local intramolecular hydrogen bonds and stabilize extended backbone conformations.

We optimized on-resin Glaser coupling diyne formation to facilitate the synthesis of a variety of macrocycles incorporated into several different peptide scaffolds. Conformational ensembles of a select series of diyne macrocycles were determined by NMR and DFT studies. We found that all variations of the diyne-braced macrocycle resulted in an extended backbone conformation, with differences in the conformation dictated by both ring size and stereochemistry. Our structural interrogation of this class of compounds provides insights into how these constraints could be used to mimic the backbone structures observed in peptide ligands, inhibitors, and natural products. To demonstrate the practical utility of this novel class of compounds, we chose to target signal peptidase 1 (SPase 1) a validated antibiotic target that binds peptide substrates in an extended conformation.[21-23]

We synthesized an array of *i, i+2* diyne-braced peptides and incorporated modifications inspired by the natural product, arylomycin, that targets SPase 1. Minimum inhibitory

A .Oxidative Glaser Macrocyclization

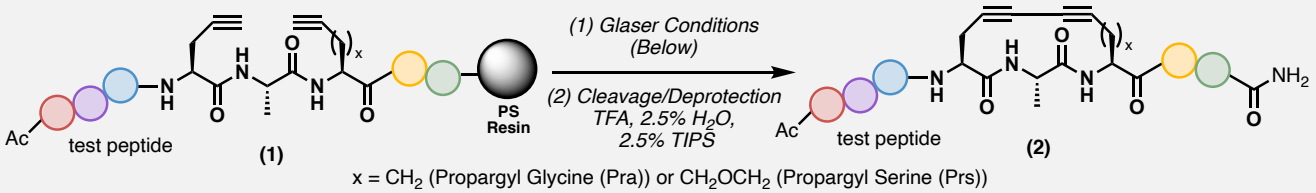

x = CH_2 (Propargyl Glycine (Pra)) or CH_2OCH_2 (Propargyl Serine (Prs))

B. Optimization Table

Entry	Temperature (°C)	Solvent	Ligand (15 eq)	Time (h)	Extra Conditions	Conversion (%) (x = CH_2/x = CH_2OCH_2)
1	4 C	DMA	2,2'-bipyridine	5 hrs	none	**79/75%**
2	r.t.	DMA	2,2'-bipyridine	5 hrs	none	**>95/>95%**
3	37 C	DMA	2,2'-bipyridine	5 hrs	none	**>95/>95%**
4	r.t.	DMSO	2,2'-bipyridine	5 hrs	none	**>95/>95%**
5	r.t.	DMF	2,2'-bipyridine	5 hrs	none	**89/92%**
6	r.t.	NMP	2,2'-bipyridine	5 hrs	none	**92/91%**
7	r.t.	2-Me THF	2,2'-bipyridine	24 hrs	none	**58/42%**
8	r.t.	THF	2,2'-bipyridine	24 hrs	none	**89/79%**
9	r.t.	ACN	2,2'-bipyridine	24 hrs	none	**86/82%**
10	r.t.	MeOH	2,2'-bipyridine	24 hrs	none	**36/56%**
11	r.t.	DCM	2,2'-bipyridine	24 hrs	none	**89/81%**
12	r.t.	DMSO	4,4'-$HOCH_2$-bipyridine	48 hrs	none	**18%/na**
13	r.t.	DMSO	4,4'-*t*Bu-bipyridine	48 hrs	none	**>95%/na**
14	r.t.	DMSO	4,4'-MeO-bipyridine	48 hrs	none	**71%/na**
15	r.t.	DMSO	Bathophenanthroline	48 hrs	none	**>95%/na**
16	37 C	DMA	2,2'-bipyridine	5 hrs	Ar purged	**19%/na**
17	37 C	DMA	2,2'-bipyridine	5 hrs	vertical	**37%/na**

Table 1 *Optimization of Glaser Coupling Conditions. All conditions include 10 eq CuCl, 15 eq specified ligand, and 20 eq DIPEA. Selected optimal conditions highlighted.*

concentration (MIC) studies revealed these "alkynomycin" variants inhibit bacterial growth at low μM MIC despite minimal design optimization. This result implies that the backbone conformation conferred by diyne-bracing alone was sufficient to mimic the activity of arylomycin and highlights the potential for further optimization of diyne macrocycles as antibiotics. Taken together these studies support peptide stretching with diyne linkages as a valuable addition to the toolbox for peptide mimicry, with broad application to molecular targets that bind peptides with extended backbone structures.

Results and Discussion

Synthetic optimization of diyne macrocycles

Although prior efforts have established the inter- and intramolecular use of the Glaser coupling in peptides,[19, 20, 24-27] we were interested in developing a robust method to access *i, i+2* peptide macrocycles quickly and efficiently **(Table 1A)**. We previously reported on-resin formation of Glaser staples for stabilization of α-helix secondary structures.[20] Pribylka et al. reported a strategy for stretching peptides via in solution formation of a diyne rod installed through perturbative peptoid linkages to the backbone.[26] Since *i, i+2* macrocycles have only 13-17 atoms, we anticipated a high level of strain and distorted bond angles, and thus predicted synthetic challenges in forming the diyne bond. However, the anticipated strain in these macrocycles is also a key design feature to limit the degrees of freedom in the peptide backbone. To facilitate the synthesis of numerous diyne peptide analogs, we optimized conditions for Glaser coupling of peptides on polystyrene beads.

Screening bipyridine ligands with an excess of CuCl and *N,N*-diisopropylethylamine in DMF yielded several candidates that efficiently promoted Cu-mediated 1,3-diyne formation and

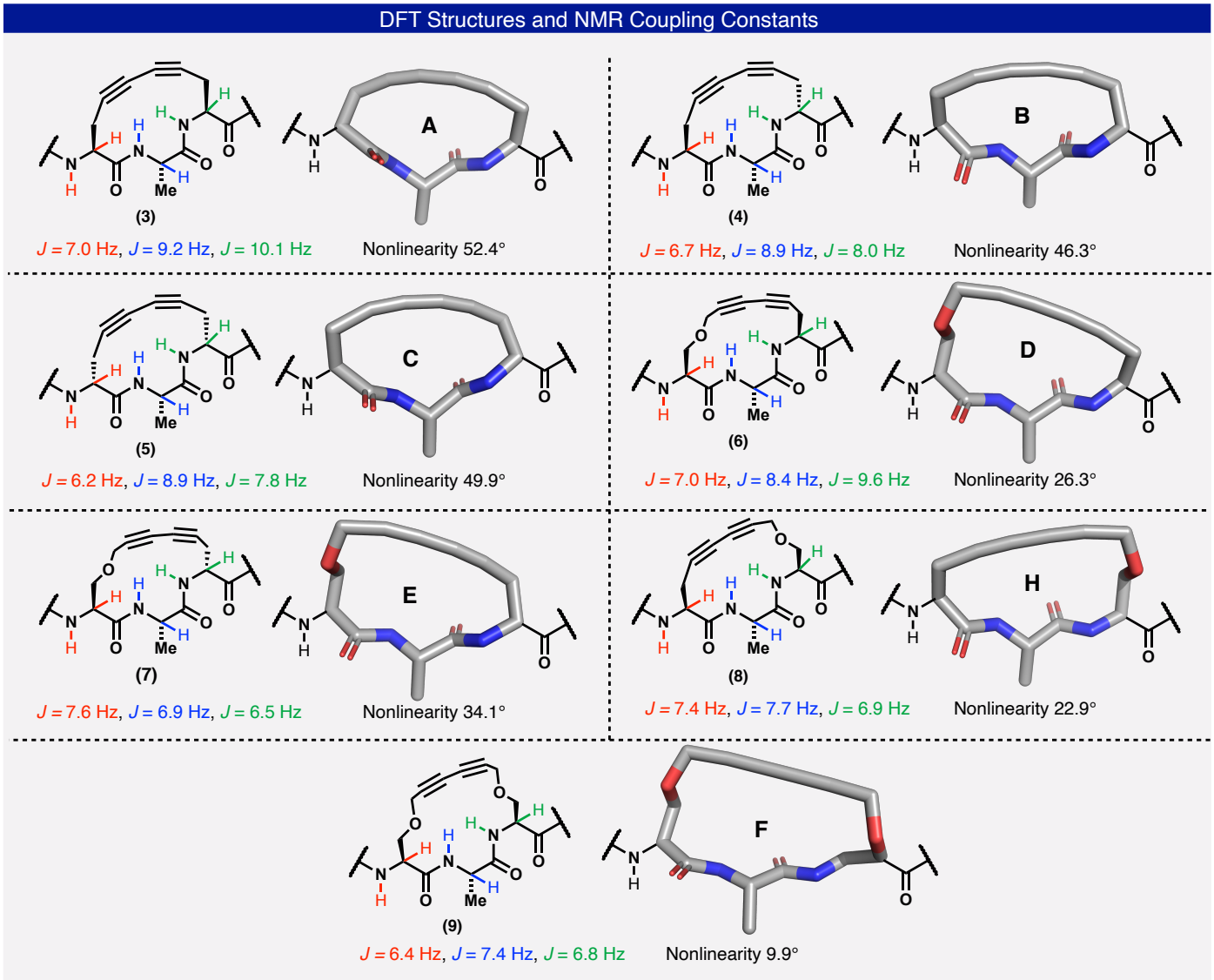

Figure 1 *Density functional theory (DFT) calculations resulted in minimized energy structures for compounds 13-, and 15-, and 17-membered rings, respectively. Notably, the backbone of these rigid macrocycles is preorganized into an extended β-strand conformation. NMR* $^{3}J_{NHC\mathrm{H}\alpha}$ *coupling constant values support these DFT structures.*

macrocycle formation on polystyrene resin (**Table 1B**). The most economical ligand, 2,2'-bipyridine, produced cyclized product in >95% conversion. Using this ligand, we screened the Glaser coupling on two compounds with different size rings, formed by incorporating propargylglycine (Pra) and propargylserine (Prs) residues, (Pra-Pra and Pra-Prs rings) with a series of solvents. Although multiple solvents were acceptable, DMA was selected as an economical and readily available solvent. Varying the reaction temperature between 4 and 37C revealed a preference for 25-37C. Saturation of the reaction mixture in air was shown to be key for the reaction, likely to facilitate re-oxidization of the Cu catalyst by O_2. Critically, the small surface area provided by a vertical shaking orientation of the Eppendorf tube limited conversion to the macrocyclic product compared to the large surface area provided by a horizontal orientation. To test this theory, we flushed the reaction vessel with argon to displace the atmosphere in the headspace and found that, indeed, conversion to the macrocyclic product was significantly reduced. Optimized conditions yielded >95% conversion to the macrocyclic product in 5 h in DMA with 2,2'-bipyridine ligand, at 37 C with horizontal shaking on both test peptide constructs (**Table 1B**). Notably, despite the anticipated strain of the *i, i+2* diyne bond, we were able to achieve similar conversions to those previously reported for stapling α-helices (>95% conversion, 3 days) in just five hours.[20]

Structural characterization of diyne macrocyles

To study the impact of the diyne macrocycle on the structural characteristics of the peptide, a series of compounds were synthesized with varied macrocycle size and stereochemistry (**Figure 1**). The seven analogues contain pairs of L- and D-propargylglycine and L-propargylserine to form rings of sizes 13 atoms, 15 atoms, and 17 atoms. These macrocycles were selected to obtain a variety of extended backbone conformations that could be used to mimic natural peptide ligands.

Structural optimization of the library of macrocycles via density functional theory (DFT) resulted in predictions of the lowest energy conformer for each ring type, shown in **Figure 1**. Notably, the diyne bond is perturbed from linearity, particularly in the smallest ring library members. The degree of nonlinearity was measured by the sum of the bond angle perturbation from the standard 180 degrees for each of the four carbons spanning the diyne. This effect is well correlated to ring size, macrocycles with a ring size of 13 members were bent 40-50 degrees out of linearity, while 15- and 17-member macrocycles were bent by 20-30 and 10 degrees, respectively (**Table S1**). Notably, the creation of a macrocycle with this level of bond distortion would likely be impossible without the binuclear copper transition state that organizes the alkynes and facilitates the formation of the diyne bond.

The DFT structures analyzed correlate well with experimental NMR data, supporting that these calculations are a good representation of the physical molecules. Coupling constants were calculated for the amide and alpha protons ($^3J_{NHCH\alpha}$) of amino acid residues within the macrocycle (propargyl-containing residues 2 and 4, and Ala3) for compounds containing each of the macrocycles in the library. According to the Karplus relation, coupling constant values typical of β-strands ($^3J_{NHCH\alpha}$ 8-10 Hz) are distinct from those of α-helices ($^3J_{NHCH\alpha}$ <6 Hz) and other protein secondary structures.[12, 28] The coupling constants measured for all library members are consistent with various extended conformations ($^3J_{NHCH\alpha}$ >6 Hz), with coupling constants for 13-membered rings generally higher than 15-membered rings. Compound **A**, the tightest macrocycle with natural stereochemistry, exhibited the highest coupling constants. Interestingly, ring size is demonstrated to be the best predictor of the extent of extended character, regardless of the stereochemistry of the ring-forming amino acids.

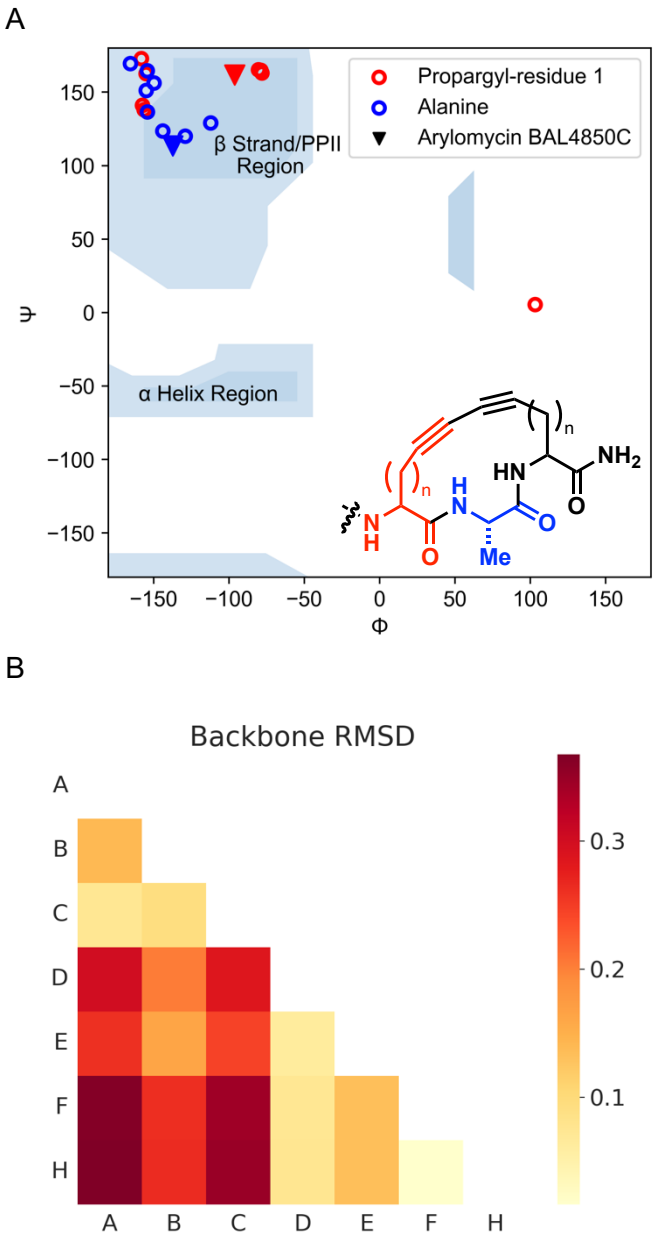

***Figure 2 A**. Dihedral angles for DFT calculated structures imply β-strand extended backbone structure. Arylomycin BAL4850C depicted by triangle for comparison **B.** Pairwise comparison of backbone structure with varied ring size*

Alkynomycin Compounds

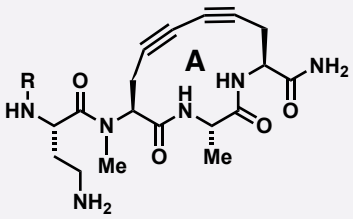

(10) *R = Dodecyl Carbamate*
(11) *R = Hexadecyl Carbamate*

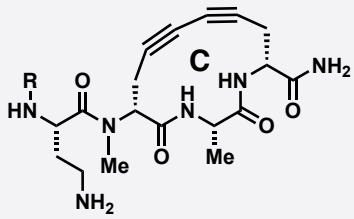

(12) *R = Dodecyl Carbamate*
(13) *R = Hexadecyl Carbamate*

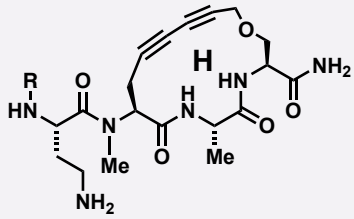

(14) *R = Dodecyl Carbamate*
(15) *R = Hexadecyl Carbamate*

Antimicrobial Activity

Compound	*S. Epidermidis*	*MRSA*	*E. Coli* $^{\Delta}$	*E. Coli*
A—C_{16}	*0.5*	*32*	*8*	*> 64*
(10)	*4*	*16*	*4*	*16*
(11)	*4*	*8*	*4*	*> 64*
(12)	*16*	*n/a*	*16*	*> 64*
(13)	*16*	*n/a*	*32*	*> 64*
(14)	*16*	*16*	*16*	*> 64*
(15)	*32*	*16*	*16*	*> 64*

Table 2 *Biological activity of alkynomycins against gram-positive and gram-negative bacteria. MICs given in ug/mL; performed in triplicate. Strains are S. epidermidis RP26a, MRSA USA 300, E. coli BAS901 (perm.), and E. coli MG1655*

The structural characteristics of the diyne motif compliment structural requirements of extended peptide structures. The distance between residues *i, i*+2 in a β-sheet is 7.0 Å, while the length of hexa-2,4-diyne, analogous to the rod installed in these peptide-based molecules, is 6.7 Å. From the DFT calculations of our library of molecules, the distance between the α-carbons of the macrocycle residues is between 6.6 and 7.0 Å (**Table S2**). Interestingly, the distance between α-carbons for 15- and 17-membered macrocycles is consistently 7.0 Å, perfectly in tune with the expected distance for β-sheet residues. Meanwhile, smaller ring sizes correlate well with further extension of the polypeptide backbone past a canonical β-strand.

All members of the designed library exhibited strong evidence of extended backbone conformation. Plotting the dihedral angles of the most abundant DFT calculated structures on a Ramachandran plot shows that the dihedral angles of the affected residues are distinctly within the β-strand/polyproline II helix region (**Figure 2A**). To further study the effect of these varied rings on the backbone structure, we computed root mean square differences (RMSD) of the DFT macrocycle structures relative to one another (**Figure 2B**). RMSD values among 13-membered macrocycles were low, supporting that the backbone conformation of these macrocycles is very similar. Interestingly, RMSD values were also low between all 15- and 17-membered macrocycles, implying that larger ring sizes confer a similar distension. These observations are consistent with our prior conclusion that ring size and extended character are correlated. Although ring size is the main predictor of similar backbone conformation, the α-carbon chirality of the ring-forming residues also affects the backbone structure. For example, the RMSD between compounds **B** and **E**, which have the same ring stereochemistry, is lower despite being 13- and 15-membered macrocycles, respectively. Manipulation of both ring size and stereochemistry can be leveraged to design superior structural matches for different target ligands.

Encouraged by this demonstration that diyne-macrocycle compounds have substantial extended-backbone character, determined by both ring size and stereochemistry, we sought to exhibit this principle by applying our platform to a protein target with translational context.

Protease inhibitors

Peptide hydrolases are a large family of enzymes that bind peptide extended conformations. Bacterial type 1 signal peptidase (SPase) is a highly conserved membrane-bound Ser-Lys dyad protease and a validated antibacterial target.[22, 23] SPase uses PPIs to recognize and cleave the N-terminal signal sequence of preproteins translocated across the cytoplasmic membrane.[29-31] Discovered in 2002,[29, 30] the arylomycins are bacteria-derived lipopeptide latent antibiotics and naturally occurring examples of ligands evolved to fit in the binding pocket of an enzyme that binds extended peptide structures. This class of molecules contain a peptide sequence bridged by a defining biaryl macrocycle that forces the peptide backbone into an extended conformation. Inspired by these natural backbone-stretchers, we used structural clues from the arylomycins to design a set of diyne-braced peptides for SPase inhibition, a class of compounds we affectionately term “alkynomycins.”

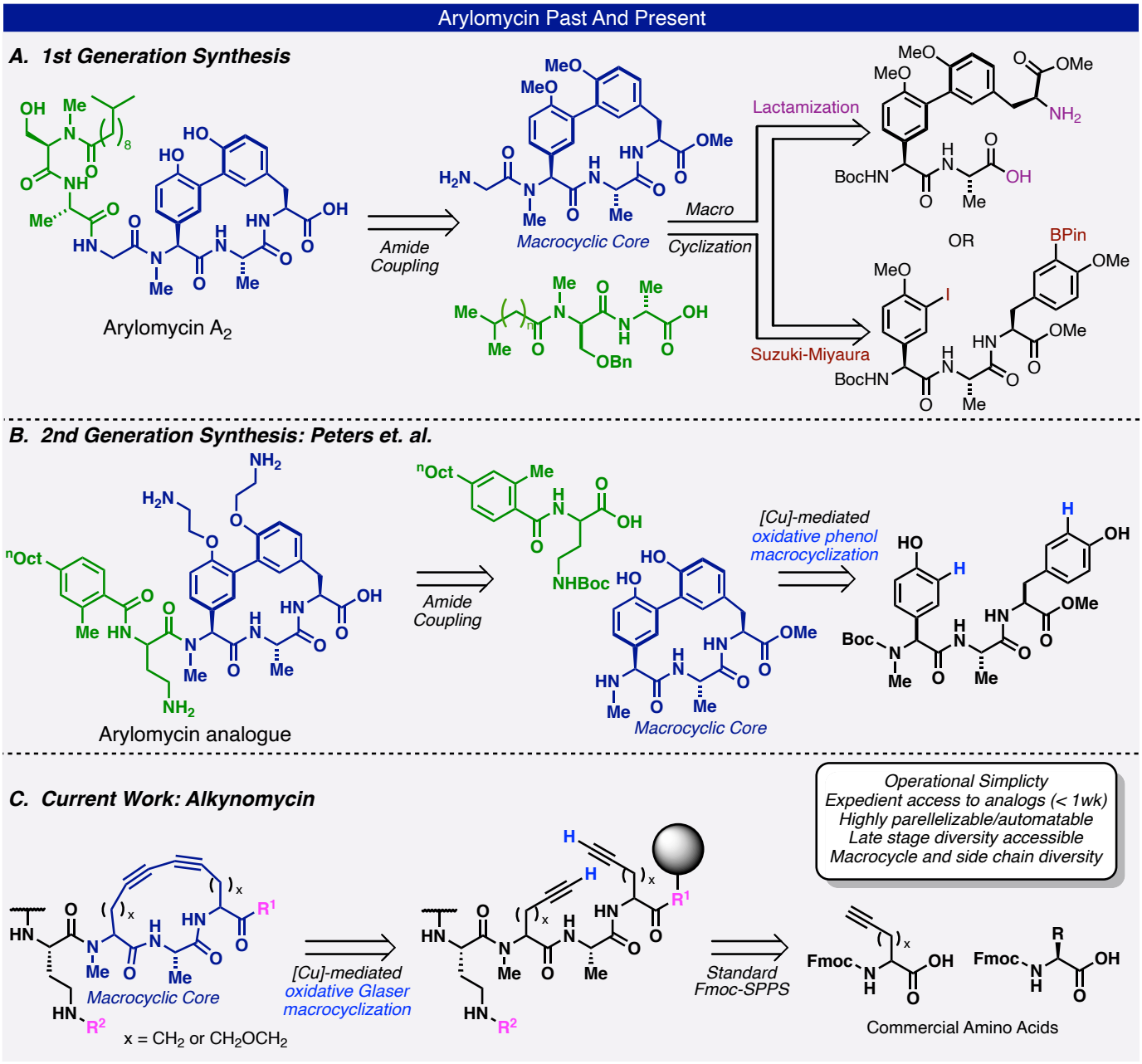

Scheme 1 A. *1st Generation synthesis of Arylomycin A_2 via Suzuki-Miyaura macrocylization.* ***B.*** *2nd Generation synthesis enabling optimization of potent arylomycin analogues via oxidative phenol macrocyclization.* ***C.*** *Current work: synthesis of alkynomycins via on-resin backbone construction and oxidative Glaser macrocyclization.*

The development of the arylomycins was initially shelved, despite activity against both Gram-positive and Gram-negative bacteria, due to narrow spectrum of activity and no activity against ESKAPE pathogens.[29, 32] Renewed interest in these compounds[33] showed that broad-spectrum activity against bacteria previously resistant to arylomycins can be reinstated via simple chemical derivatization of the lipid tail that renders the resistance-conferring mutation in SPase irrelevant,[34] leading to recent syntheses of a number of novel and potent analogues.[23, 33, 35-37]

Structural analyses of SPase in complex with arylomycin confirm that the SPase-binding region of the arylomycin class of antibiotics adopts an extended peptide backbone (**Figure 3A**).[21] Since the biaryl moiety is solvent exposed without productive interactions with the highly conserved catalytic pocket, its primary structural role is to preorganize the peptidic SPase binding motif.[38, 39] A comparison of the dihedral angles in DFT calculated structures of our library of macrocycles with those of arylomycin compound
BAL4850C showed good correlation (**Figure 2**). Like the arylomycin compounds, dihedral angles of the alanine and N-terminal residues, which are constrained by the ring, are

consistent with a β-strand extended conformation. Similarly, NMR coupling constants for arylomycin compounds[35] are comparable to those of the alkynomycins, particularly for the 13-membered diyne-braced rings. Indeed, the further extended backbone conformation of the 13-membered diyne-braced macrocycles is structurally analogous to the extension native to the arylomycins.

Using the designed library of diyne-braced macrocycles and inspiration from arylomycin-class compounds, a preliminary set of analogues was generated for evaluation in an MIC assay against a panel of gram-positive and gram-negative bacteria **Table 2, Table S3**. An *N*-methyl was installed on the N-terminal ring residue, as this group has previously been shown to be required for activity in analogous arylomycin compounds.[36] In accordance with previous synthetic optimization, the ring was followed by diaminobutyric acid instead of lysine.[23] The N-terminus was functionalized with commercially available dodecyl- and hexadecyl-carbamate tails.

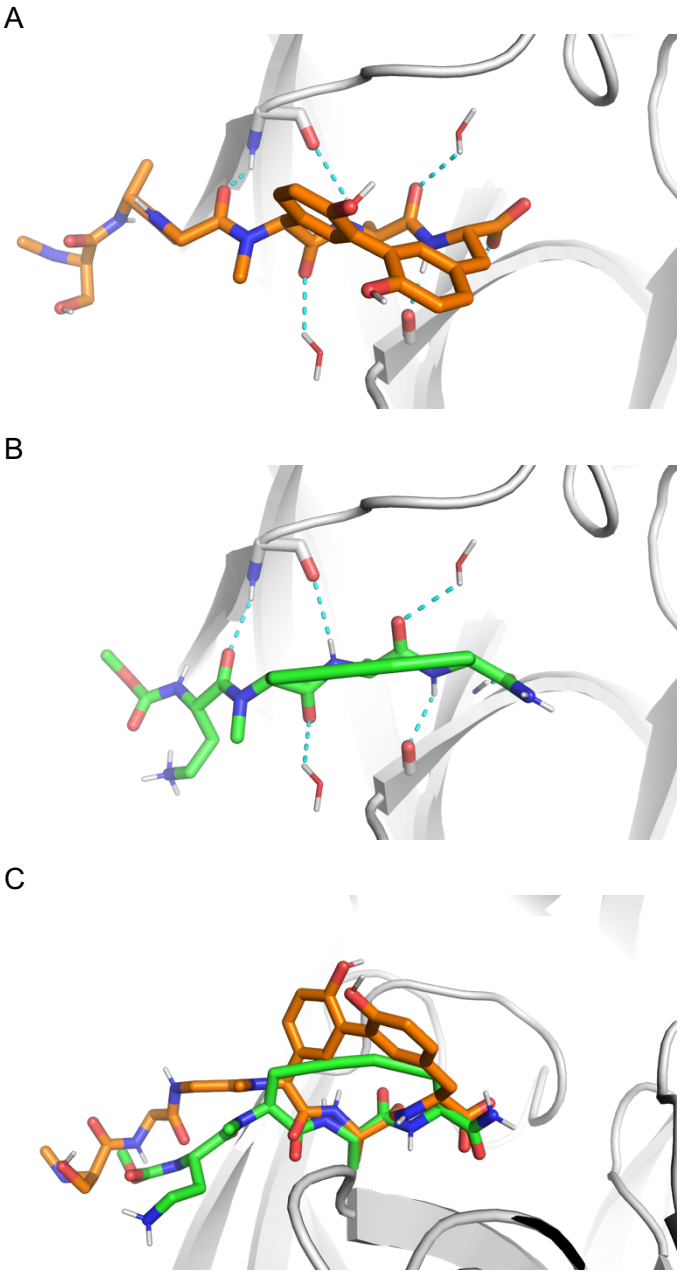

Figure 3 A. *Arylomycin A_2 co-crystalized with E. coli type 1 signal peptidase* ***B.*** *Alkynomycin compound* ***A*** *docked in E. coli type 1 signal peptidase* ***C.*** *Superposition of Arylomycin A_2 and Alkynomycin compound* ***A***

The activities of the most efficacious compounds are summarized in **Table 2**. Compounds with ring types **A**, **C**, and **H**, having 13-, 13-, and 15-membered macrocycles, respectively, had the highest activity of the alkynomycins tested. Strikingly, without any further optimization, the two alkynomycin compounds with ring type **A** performed comparably (within a factor of 2) to previously-reported Arylomycin A–C_{16}[34] against *MRSA,* and both permeabilized and non-permeabilized *E. coli*. Despite being less potent than Arylomycin A-C_{16} for *S. epidermidis,* both alkynomycins with ring type **A** were still highly potent, and alkynomycin **A12** even had activity against non-permeabilized *E. coli.* Consistent with the structure activity relationship of arylomycin, *N*-methylation and macrocyclization were both essential for activity of the alkynomycins (**Table S4**). This dependence of activity on key elements of the arylomycin backbone suggests that the alkynomycins and arylomycins share a common mechanism of action. To further investigate this commonality, a flexible macrocycle docking protocol was applied to dock a methylcarbamate analog with ring type **A** against a structure of E. coli type 1 signal peptidase co-crystalized with arylomycin A_2.[21] The results show that the diyne-stretched backbone of alkynomycin **A** docks with a binding mode strikingly similar to the biaryl-stretched backbone of arylomycin A_2 (**Figure 3**). The docked amide backbone conformation induced by ring type **A** very closely reproduces the hydrogen bond pattern of the bound arylomycin, including interactions with bridging waters.

Taken together, these results support that the alkynomycin **A** scaffold can be considered a first-generation lead compound that should benefit from the rich structure function data that has been collected for the arylomycin scaffolds. The alkynomycin compounds tested mimic the structure of Arylomycin A–C_{16} most closely, while studies have already shown that modifications at the C-terminus, the N-terminal lipid, and *N*-methylation sites drastically improve potency. Incorporation of these known modifications, or screening for further modifications at these sites, has the potential to refine the activity of alkynomycin antibiotics.

Although alkynomycins with ring types **A** and **C** share the same ring size, compounds with ring type **A** had significantly greater potency. Interestingly, alkynomycin **B**, which also has the same ring size as **A** and **C** and significant extended backbone structure suggested by NMR, was inactive. Similarly, despite having the same ring size, compounds with ring types **D** and **E** were far less active than ring type **H** compounds. Meanwhile the 17-membered macrocycle **F** was considered inactive (>64 ug/mL). These results emphasize the possibility of creating unique ligands that match the requirements of distinctive binding sites by varying the identity of the macrocycle. Screening larger libraries of molecules of this class has the potential to discover precisely tailored fits for a broad array of targets.

Access to low-molecular weight diyne-braced β-strand mimics with designed-fit for target proteins is promising for the development of therapeutics to target the many diseases mediated by PPIs. Synthetic access to diverse analogues and

large quantities of natural products is often limited by availability of starting materials, low yields, and difficult chemical steps. Active pursuit of the arylomycins has established viable synthetic routes, **Scheme 1**.[23, 33, 35-37] In contrast, diyne-bracing eliminates the synthetically challenging biaryl ring while maintaining the SPase-recognized extended backbone conformation. The SPPS-compatible route to the alkynomycins can enable rapid generation of diverse and efficacious analogues with minimal purification steps.

Antibiotic resistance poses a serious global health risk and contributes to an increasing number of mortalities each year.[40-43] With developments of new classes of antibiotics stalled in the last decades, the need for new strategies to target bacteria and stave off infection has become pressing. The arylomycins are not the sole example of Nature using peptide stretching for antibiotics. Darobactin, a recently discovered bismacrocyclic heptapeptide antibiotic that is selective for Gram-negative bacteria, is stretched by two intersecting macrocycles into a β-strand structure allowing it to bind along the exposed face of a β-sheet in its protein target,[44, 45] highlighting a distinct binding modality for stretched peptides. Applying inspiration from the mechanism of action of macrocyclic natural product antibiotics has the potential to uncover new classes of stretched-backbone peptide antibiotics. The present strategy for simplifying synthetic routes to stretched backbone peptides using diyne bracing should be broadly applicable in the development and high throughput screening of novel efficacious antimicrobials.

Conclusion

Here we report the efficient on-resin synthesis of a series of compounds characterized by rigid diyne ring systems. The establishment of this method facilitates access to low molecular weight (< 300 Da) mimics of β-strand and PPII helix motifs abundant in natural protein-peptide ligand complexes, with minimal chemical perturbations to the peptide sequence. Both theoretical DFT calculations and experimental NMR data indicate significant extended backbone character in these compounds controlled by ring size and stereochemistry. Using this synthetic control to access different extended structures can enable the creation of molecules with designed fit for the protein of interest. Since this method can be performed on-resin, we foresee this chemistry enabling the efficient generation of large chemical diversity. The alkynomycins, a new class of *i, i+2* diyne-braced antimicrobial compounds, illustrate the promise of diyne-braced peptides for new opportunities to modulate PPIs.

Implementation of our diyne peptide-bracing strategy exemplifies its utility in protease inhibitor design to address challenges in human health. Since a significant proportion of the proteome is involved in interactions with IDRs, this strategy for accessing low molecular weight peptide-based extended structures holds great promise for addressing previously “undruggable” targets. Additionally, the diyne bond is inherently Raman sensitive[46] and can be reacted to form further functionalized analogues.[47, 48] We anticipate the broad application of this method since it is both and compatible with standard SPPS and drug discovery methods and consistent with inspiration from natural products like arylomycin and darobactin, where the mechanism of action is driven by the binding conformation of the peptide backbone.[29, 30, 45] Stretching peptides via diyne-bracing promises to open doors for the development of new modulating compounds compatible with the vast extended section of the proteome using rigidly extended-backbone peptides.

Acknowledgements:

The authors would like to acknowledge the Automated Synthesis Facility at Scripps Research, particularly Brittany B. Sanchez. Floyd E. Romesberg provided inspiration and helpful discussions and Marco Mravic provided critical comments. The present work was financially supported by the National Science Foundation Graduate Research Fellowships Program DGE-1842471 (Z.C.A.), Natural Sciences and Engineering Research Council of Canada Postdoctoral Fellowship 5577584-2021 (S.C.), and the National Institutes of Health R01GM069832 (S.F.) and R21GM132787 (P.E.D.).

References:

1. Gsponer J, Babu MM. The rules of disorder or why disorder rules. *Prog Biophys Mol Biol* 2009, **99**(2-3)**:** 94-103.

2. Loughlin WA, Tyndall JDA, Glenn MP, Fairlie DP. Beta-Strand Mimetics. *Chem Rev* 2004, **104:** 6085-6117.

3. Nevola L, Giralt E. Modulating protein-protein interactions: the potential of peptides. *Chem Commun (Camb)* 2015, **51**(16)**:** 3302-3315.

4. Uversky VN, Dunker AK. Understanding protein non-folding. *Biochim Biophys Acta* 2010, **1804**(6)**:** 1231-1264.

5. Oldfield CJ, Dunker AK. Intrinsically disordered proteins and intrinsically disordered protein regions. *Annu Rev Biochem* 2014, **83:** 553-584.

6. Gonzalez MW, Kann MG. Chapter 4: Protein interactions and disease. *PLoS Comput Biol* 2012, **8**(12)**:** e1002819.

7. Coyne AG, Scott DE, Abell C. Drugging challenging targets using fragment-based approaches. *Curr Opin Chem Biol* 2010, **14**(3)**:** 299-307.

8. Winter A, Higueruelo AP, Marsh M, Sigurdardottir A, Pitt WR, Blundell TL. Biophysical and computational fragment-based approaches to targeting protein-protein interactions: applications in structure-guided drug discovery. *Q Rev Biophys* 2012, **45**(4)**:** 383-426.

9. Goudreau N, Brochu C, Cameron DR, Duceppe JS, Faucher AM, Ferland JM*, et al.* Potent Inhibitors of the Hepatitis C Virus NS3 Protease: Design and Synthesis of Macrocyclic Substrate-Based Beta-Strand Mimics. *J Org Chem* 2004, **69:** 6185-6201.

10. Stigers KD, Soth MJ, Nowick JS. Designed molecules that fold to mimic protein secondary structures. *Current Opinion in Chemical Biology* 1999, **3:** 714-723.

11. Sarnowski MP, Kang CW, Elbatrawi YM, Wojtas L, Del Valle JR. Peptide N-Amination Supports beta-Sheet Conformations. *Angew Chem Int Ed Engl* 2017, **56**(8)**:** 2083-2086.

12. Hill TA, Shepherd NE, Diness F, Fairlie DP. Constraining cyclic peptides to mimic protein structure motifs. *Angew Chem Int Ed Engl* 2014, **53**(48)**:** 13020-13041.

13. Pelay-Gimeno M, Glas A, Koch O, Grossmann TN. Structure-Based Design of Inhibitors of Protein-Protein Interactions: Mimicking Peptide Binding Epitopes. *Angew Chem Int Ed Engl* 2015, **54**(31)**:** 8896-8927.

14. Nowick JS, Chung DM, Maitra K, Maitra S, Stigers KD, Sun Y. An Unnatural Amino Acid that Mimics a Tripeptide Beta-Strand and Forms Beta-Sheetlike Hydrogen-Bonded Dimers. *J Am Chem Soc* 2000, **122**(7654-7661).

15. Tsai JH, Waldman AS, Nowick JS. Two New β-Strand Mimics. *Bioorganic and Medicinal Chemistry* 1999, **7:** 29-38.

16. Kang CW, Sun Y, Del Valle JR. Substituted Imidazo[1,2-a]pyridines as Beta-Strand Peptidomimetics. *Organic Letters* 2012, **14**(24)**:** 6162-6165.

17. Kang CW, Sarnowski MP, Ranatunga S, Wojitas L, Metcalf RS, Guida WC*, et al.* β-Strand mimics based on tetrahydropyridazinedione (tpd) peptide stitching. *Chem Commun (Camb)* 2015, **51**(90)**:** 16259-16262.

18. Reid RC, March DR, Dooley MJ, Doug AB, Abbenante G, Fairlie DP. A Novel Bicyclic Enzyme Inhibitor as a Consensus Peptidomimetic for the Receptor-Bound Conformations of 12 Peptidic Inhibitors of HIV-1 Protease. *J Am Chem Soc* 1996, **118**(36)**:** 8511-8517.

19. Silvestri AP, Cistrone PA, Dawson PE. Adapting the Glaser Reaction for Bioconjugation: Robust Access to Structurally Simple, Rigid Linkers. *Angew Chem Int Ed Engl* 2017, **56**(35)**:** 10438-10442.

20. Cistrone PA, Silvestri AP, Hintzen JCJ, Dawson PE. Rigid Peptide Macrocycles from On-Resin Glaser Stapling. *ChemBioChem Communications* 2018, **19:** 1031-1035.

21. Paetzel M, Goodall JJ, Kania M, Dalbey RE, Page MG. Crystallographic and biophysical analysis of a bacterial signal peptidase in complex with a lipopeptide-based inhibitor. *J Biol Chem* 2004, **279**(29)**:** 30781-30790.

22. Tan YX, Romesberg FE. Latent antibiotics and the potential of the arylomycins for broad-spectrum antibacterial activity. *MedChemComm* 2012, **3**(8)**:** 916-925.

23. Smith PA, Koehler MFT, Girgis HS, Yan D, Chen Y, Chen Y*, et al.* Optimized arylomycins are a new class of Gram-negative antibiotics. *Nature* 2018, **561**(7722)**:** 189-194.

24. Okorochenkov S, Krchnak V. Application of Glaser-Hay Diyne Coupling To Constrain N(alpha)-Amino Acid Amides via a N-N Bridge. *ACS Comb Sci* 2019.

25. Verlinden S, Geudens N, Van Holsbeeck K, Mannes M, Martins JC, Verniest G*, et al.* The 1,3-diyne linker as a rigid "i,i+7" staple for alpha-helix stabilization: Stereochemistry at work. *J Pept Sci* 2019, **25**(7)**:** e3194.

26. Přibylka A, Krchňák V. An Alkyne Rod to Constrain a Peptide Backbone in an Extended Conformation. *European Journal of Organic Chemistry* 2018, **2018**(34)**:** 4709-4715.

27. Lampkowski JS, Villa JK, Young TS, Young DD. Development and Optimization of Glaser-Hay Bioconjugations. *Angew Chem Int Ed Engl* 2015, **54**(32)**:** 9343-9346.

28. Case DA, Dyson JH, Wright PE. Use of Chemical Shifts and Coupling Constants in Nuclear Magnetic Resonance Structural Studies on Peptides and Proteins. *Methods in Enzymology* 1994, **239:** 392-416.

29. Schimana J, Gebhardt K, Höltzel A, Schmid DG, Süssmuth R, Müller J*, et al.* Arylomycins A and B, New Biaryl-bridged Lipopeptide Antiobiotics Produced by Streptomyces sp. Tü 6075. *The Journal of Antibiotics* 2002, **55**(6)**:** 565-570.

30. Höltzel A, Schmid DG, Nicholson GJ, Stevanovic S, Schimana J, Gebhardt K*, et al.* Arylomycins A and B, New Biaryl-bridged Lipopeptide Antibiotics Produced by Streptomyces sp. Tü 6075. *The Journal of Antibiotics* 2002, **55**(6)**:** 571-577.

31. Auclair SM, Bhanu MK, Kendall DA. Signal peptidase I: cleaving the way to mature proteins. *Protein Sci* 2012, **21**(1)**:** 13-25.

32. Kulanthaivel P, Kreuzman AJ, Strege MA, Belvo MD, Smitka TA, Clemens M*, et al.* Novel lipoglycopeptides as inhibitors of bacterial signal peptidase I. *J Biol Chem* 2004, **279**(35)**:** 36250-36258.

33. Wu ZC, Boger DL. The quest for supernatural products: the impact of total synthesis in complex natural products medicinal chemistry. *Nat Prod Rep* 2020, **37**(11)**:** 1511-1531.

34. Smith PA, Roberts TC, Romesberg FE. Broad-spectrum antibiotic activity of the arylomycin natural products is masked by natural target mutations. *Chem Biol* 2010, **17**(11)**:** 1223-1231.

35. Peters DS, Romesberg FE, Baran PS. Scalable Access to Arylomycins via C-H Functionalization Logic. *J Am Chem Soc* 2018, **140**(6)**:** 2072-2075.

36. Roberts TC, Smith PA, Cirz RT, Romesberg FE. Structural and Initial Biological Analysis of Synthetic Arylomycin A2. *J Am Chem Soc* 2007, **129:** 15830-15838.

37. Wong N, Petronijevic F, Hong AY, Linghu X, Kelly SM, Hou H*, et al.* Stereocontrolled Synthesis of Arylomycin-Based Gram-Negative Antibiotic GDC-5338. *Org Lett* 2019, **21**(22)**:** 9099-9103.

38. Luo C, Roussel P, Dreier J, Page MG, Paetzel M. Crystallographic analysis of bacterial signal peptidase in ternary complex with arylomycin A2 and a beta-sultam inhibitor. *Biochemistry* 2009, **48**(38)**:** 8976-8984.

39. Liu J, Luo C, Smith PA, Chin JK, Page MG, Paetzel M*, et al.* Synthesis and characterization of the arylomycin lipoglycopeptide antibiotics and the crystallographic analysis of their complex with signal peptidase. *J Am Chem Soc* 2011, **133**(44)**:** 17869-17877.

40. Antimicrobial Resistance: Global Report on Surveillance. In: Organization WH (ed). 2014.

41. O'Neill J. Tackling Drug-Resistant Infections Globally: Final Report and Recommendations. 2016.

42. Murray CJL, Ikuta KS, Sharara F, Swetschinski L, Robles Aguilar G, Gray A*, et al.* Global burden of bacterial antimicrobial resistance in 2019: a systematic analysis. *The Lancet* 2022.

43. Mahaney AP, Franklin RB. Persistence of wastewater-associated antibiotic resistant bacteria in river microcosms. *Sci Total Environ* 2022**:** 153099.

44. Nesic M, Ryffel DB, Maturano J, Shevlin M, Pollack SR, Gauthier DR*, et al.* Total Synthesis of Darobactin A. *Journal of the American Chemical Society* 2022, **144**(31)**:** 14026-14030.

45. Imai Y, Meyer KJ, Iinishi A, Favre-Godal Q, Green R, Manuse S*, et al.* A new antibiotic selectively kills Gram-negative pathogens. *Nature* 2019, **576**(7787)**:** 459-464.

46. Yamakoshi H, Dodo K, Palonpon A, Ando J, Fujita K, Kawata S*, et al.* Alkyne-tag Raman imaging for visualization of mobile small molecules in live cells. *J Am Chem Soc* 2012, **134**(51)**:** 20681-20689.

47. Asiri AM, Hashmi AS. Gold-catalysed reactions of diynes. *Chem Soc Rev* 2016, **45**(16)**:** 4471-4503.

48. Shi W, Lei A. 1,3-Diyne chemistry: synthesis and derivations. *Tetrahedron Letters* 2014, **55**(17)**:** 2763-2772.

49. Schrödinger Release 2019-2: MacroModel. New York, NY: Schrödinger, LLC; 2019.

50. Frisch MJ, Trucks GW, Schlegel HB, Scuseria GE, Robb MA, Cheeseman JR*, et al.* Gaussian 16, Revision B.01. Wallingford CT; 2016.

51. Methods for dilution antimicrobial susceptiblity tests for bacteria that grow aerobically. In: Institute CaLS, editor. Wayne, PA; 2011.

Methods

Synthetic Methods

General Solid-Phase Peptide Synthesis (SPPS) Procedure All peptides were chain assembled on Rink Amide polystyrene resin (0.64 mmol/gram) or Rink-Amide TentaGel resin (loading 0.2 mmol/g, Rapp Polymere GmbH) by individual hand couplings. All standard amino acid couplings were carried out with the equivalent ratio of [5]:[5]:[7.5] of [Fmoc-protected amino acid]:[0.4 M HATU in DMF]:[DIPEA] for 20 minutes following standard SPPS protocol with N-terminal Fmoc-protection. Propargyl containing amino acids were coupled by hand using the equivalent ratio of [2.5]:[2.5]:[3.8] of these components for 90 minutes, and followed by a qualitative ninhydrin test to ensure complete coupling.

***N*-Methylation** After peptide assembly of the macrocycle ring, N-methylation of residue 3 was performed on-resin. Resin was treated twice with [1]:[1] DBU:EtTFA in DMF for 30 min, and then checked with a qualitative ninhydrin test to ensure complete protection of the N-terminus. An equivalent ratio of [5]:[10] [PPh_3]:[MeOH] in DCM was added to resin in a closed tube with stopcock. 5 equivalents DIAD was added last and the tube was vented, then shaken for 1 hour. This procedure was repeated until a test cleavage showed good conversion to the methylated N-terminus. The protecting group was cleaved with 20 equivalents of $NaBH_4$ in 1:1 MeOH:DCM. The amino acid directly following this step was coupled twice by standard SPPS protocol.

On-resin Glaser Coupling To a 15 mL Falcon tube was added CuCl (100 mg, 1 mmol, 10 equiv.), 2,2'-bipyridine ligand (165 mg, 1.5 mmol, 15 equiv.), and 0.1 mmol of washed Fmoc-deprotected peptide-loaded resin, prior to the addition of any alkyl tails. The mixture was briefly vortexed to mix the Cu and ligand. To this tube was added 5 mL DMA, followed by 175 µL DIEA (1 mmol, 10 equiv.). The tube was parafilmed and placed sideways in a secondary container to reduce settling of compounds to the bottom of the tube and improve interaction of the solution with O_2 in the headspace. The tube was incubated at 37 C with shaking at 180 rpm for 5 hrs. Following the stapling reaction, the resin was washed with DMF and piperidine and subjected to either continued synthesis (i.e. coupling of alkyl tail) or standard TFA cleavage conditions for SPPS procedure.

Chloroformate Coupling Alkyl chloroformate tails were appended by adding DMAP (1 equiv.) to a mixture of resin and chloroformate (5 equiv.) in 1:1 DCM/DMF (2 mL total), stirring for 1 hour, and subsequent flow washing with DMF. Coupling completion was ensured by a qualitative ninhydrin test.

Cleavage and purification Peptides were cleaved from resin within 48 hours of the formation of the diyne brace to prevent undesired copper-catalyzed modifications observed to occur on-resin. Peptides proceeded to standard cleavage from resin using [2.5]:[2.5]:[95] TIPS:H2O:conc. TFA at 45 C for 4 hours. The TFA was reduced via rotovap then added to an excess of 30% B and lyophilized. The crude peptide thus obtained was purified via preparative reversed-phase HPLC (RP-HPLC) using optimized gradients (**Supporting Information**).

Density Functional Theory Modeling

A Monte Carlo conformational search undertaken using the OPLSe3 forcefield and simulated water solvent (GB/SA) using Macromodel v12.[49] The selected conformers (< 3 kcal/mol of the global minimum) were optimized by density functional theory (DFT) calculations at the B3LYP/6-31G(d,p) level with PCM implicit solvent model for water using Gaussian software G16W.[50] A single point energy of the optimized conformers was calculated using M062X/6-31+g(d,p) with PCM implicit solvent model for water and duplicate conformers and conformers with >3 Kcal/mol of the global minimum were removed. Finally, single point free energy of the optimized conformers was calculated using M062X/6-31+G(d,p) with PCM implicit solvent model for water were used to scale the calculated NMR parameters relative to their Boltzmann population and the vibrational frequencies where checked for a true minimum, i.e. no negative frequencies and this energy was used to calculated the Boltzmann populations for each compound.

Nuclear Magnetic Resonance Spectroscopy

Two main approaches were taken when preparing the braced peptide products for NMR analyses. Braced peptides not containing a lipid tail (0.8 – 1.4 mg) were dissolved in 500 µL H_2O and 50 µL D_2O and analyzed in 5 mm tubes on a 700 MHz Bruker Avance III spectrometer equipped with a cryoprobe. Alkynomycin analogues (1.8 – 2.2 mg) were dissolved in 150 µL DMSO-d_6 and analyzed on a 600 MHz Bruker spectrometer equipped with either a 5 mm CPQCI or CPDCH cryoprobe in 3 mm tubes. As all compounds were purified as TFA salts, pH of solutions were adjusted to within the range 4.6 – 5.3 and scans were obtained at 298 K. Water suppression was achieved by excitation sculpting during proton spectral acquisition.

^{1}H homonuclear data included 2D total correlation spectroscopy (TOCSY) with a mixing time of 80 ms, rotating-frame Overhouser effect spectroscopy (ROESY) with a mixing time of 100 ms, and nuclear Overhauser effect spectroscopy (NOESY) with a mixing time of 300 ms. The homonuclear data were recorded with a sweep width of 10 or 12 ppm with 4k data points in the direct and 512 increments in the indirect dimension. Heteronuclear single quantum coherence (HSQC) data were also recorded at natural abundance. The ^{1}H-^{13}C HSQC spectra were recorded with 2k data points over a sweep width of 10 or 12 ppm in the direct dimension, and 280 increments over a sweep width of 80 ppm, covering the aliphatic carbon region, in the indirect dimension. The ^{1}H-^{15}N HSQC spectra were recorded with 2k data points over a sweep width of 10 ppm in the direct dimension, and 128 increments over a sweep width of 32 ppm in the indirect dimension for the group of peptides.

All data were collected using Topspin 4.0.6 (Bruker), processed with MestReNova 14.2.1 (Maestrelab Research). Water solvated samples were referenced to internal DSS at 0.0 ppm and DMSO samples were referenced to residual solvent peak at 2.50 ppm.

Minimum Inhibitory Concentration Assay

MICs were performed in accordance with the broth microdilution protocol from the Clinical and Standards Laboratory Institute.[51]

Alkynomycins were dissolved in DMSO and two-fold serial dilutions were made across a 96-well plate containing Muller-Hinton (MH) broth. One plate was used for each indicator organism, and each well reached a final inoculum of 5×10^5 colony forming units per mL. Using OD_{600} readings normalized to a negative control, MICs were recorded as the lowest concentration at which growth was inhibited after a 24 h incubation at 37 °C. Controls were included on each plate to ensure peptide and media sterility. MICs are reported in **Table 2** and **Table S3, S4** as an average of at least three independent trials.

Indicator organisms were stored at -80 °C as glycerol stocks. Each organism was streaked onto tryptic soy agar and grown for 24 h at 37 °C. Single colonies were picked and used to inoculate MH broth. Bacteria culture was diluted to reach an OD_{600} of 0.015 prior to being used for MIC assays.

Molecular Docking

The co-crystallized ligand was removed from the structure (1t7d),[21] with crystallographic waters retained. The structure was prepared for docking using AutoDockTools. Grid maps were prepared using AutoGrid v4.2.6 with 30 Å in each dimension and 0.375 Å spacing. The ligand was prepared with terminal alkynes. “Glue” atoms (G0 type) appropriate for macrocyclic docking were placed 1.5 Å from the end of each of alkyne, and the terminal carbon of the alkynes were typed CG0. Docking was performed using AutoDock-GPU v1.5.3. 20 independent genetic algorithm runs were performed, with an AutoStop triggered by an energy standard deviation cutoff at 0.15 kcal/mol. The best scored pose was used for structural analysis.